

Front-End Circuit in Electrical Resistance Tomography (ERT) for Two-Phase Liquid and Gas Imaging

F. R. Mohd Yunus^a, R. Abdul Rahim^{a*}, Suzanna Ridzuan Aw^b, N. M. Nor Ayob^a, M. P. Jayasuman^a, M. F. Jumaah^a

^aProcess Tomography & Instrumentation Research Group (PROTOM-i), Faculty of Electrical Engineering, Universiti Teknologi Malaysia, 81310 UTM Johor Bahru, Johor, Malaysia

^bFaculty of Electrical & Automation Engineering Technology, Terengganu Advance Technical Institute University College (TATIUC), Jalan Panchor, Telok Kalong, 24000, Kemaman, Terengganu, Malaysia

*Corresponding author: ruzairi@fke.utm.my

Article history

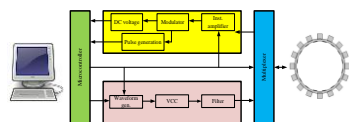
Received :5 February 2014

Received in revised form :

7 April 2014

Accepted :20 May 2014

Graphical abstract



Abstract

A steady and precise Voltage Control Current Source (VCCS) with broad bandwidth plays a very important role in the quality of final images for the Electrical Resistance Tomography (ERT) system. Therefore, a model of current source is proposed in the paper which implement advanced Howland current pump as VCCS. The model are simulated through a software named *multisim*, and the simulation results show the proposed high-speed operational amplifier (op-amp) LM7171 is capable to produce constant output current at 10 mA (peak) when the frequency changes between 1 kHz to 500 kHz with load varies from 10 Ω to 1 k Ω . A two-dimensional (2D) simulation was performed using COMSOL and the results showed that the model is capable to detect air bubble (radius=10 mm) in a two-phase liquid and gas. The result presented with opposite excitation method with 150 kHz current at 10 mA. The measurement of boundary potentials are significantly influenced by bubble positions particularly towards the boundary. They are hoped to provide useful approaches for the design of practical and low-cost VCCS in ERT system.

Keywords: Electrical resistance tomography; opposite excitation; COMSOL; Howland current pump circuit

© 2014 Penerbit UTM Press. All rights reserved.

1.0 INTRODUCTION

Electrical resistance tomography (ERT) is non-intrusive method based upon a reconstruction profile of electrical conductivity inside a medium of interests from measurement made on its boundary [1]. Electrical resistance tomography (ERT) is a specific form of soft-field process tomography technique. As an on-line measurement technique possessing advantages of visualization, non-invasion, low cost, and non-radiation, ERT has become an accepted measuring technique in process of engineering applications [2]. The technique has been used in many fields such as petroleum, chemical, metallurgy and pharmacy etc. especially in the measurement of two-phase multi-phase flows. The objective of ERT is to achieve cross section images through set of boundary sensors array to obtain the real-time distribution of electric materials with a contrast in conductivity. As the distribution of conductivity changes, the distribution of current field inside vessel also changes, hence the changes of the electrical potential occurs, and finally the changes of the boundary voltage measurements. The changes of the conductivity changes, in other words, the medium distribution can be identified if the conductivity distribution of the sensing field is acquired. With a

lot of advantages, such as 2D and 3D visualization, high speed, low cost and radiation hazard free, ERT is a promising technique to monitor widely existing industrial processes with conductive continuous phase flow [3].

Typical ERT structure is composed of three basic parts: sensors, signal conditioning, data acquisition system (DAS) and image reconstruction system [4]. Unlike the electrical capacitance tomography (ECT) the electrodes in ERT must have continuous electrical contact with the conductive liquid inside the vessel. Most industrial process applications implement metallic electrodes fabricated from aluminium, silver, gold, stainless steel and platinum or other suitable materials exhibiting certain properties. As rule of thumb the conductivity of sensor electrodes must have higher conductivity properties compared to the liquid conductivity. Some of the essential properties include low cost; ease of fabrication and installation; good electrical conduction; resistance to corrosion and abrasion. The data acquisition system (DAS) performs a series of functions such as waveform generation and synchronisation; multiplexer switching control, measurements and de-modulation. Some of the common data collection strategies suited to a single-current source/sink-drive stage includes: the adjacent strategy; the opposite strategy; the diagonal strategy and the conducting boundary strategy. A

reconstruction algorithm is applied to determine the internal distribution of resistivity within the process vessel from measurements acquired from an array of electrodes mounted on its periphery.

In this paper, rectangular electrodes were selected initially for the simulation study using COMSOL. In simulation purposes, an excitation current of 10 mA with 150 kHz has been implemented with 12 mm rectangular electrodes array. The authors developed a two-dimensional (2D) electrical resistance tomography (ERT) model using finite element method (FEM) with COMSOL software. Using 2D numerical analysis with COMSOL, the authors analysed capability influence of 10 mA current excitation on the distribution of the sensing field particularly in two-phase liquid and gas in vessel with inner diameter of 100 mm. This gives rise to even distribution of currents, leading to good image characterization [5] as illustrated in Figure 2

Typical ERT structure is composed of three basic components: sensors, signal conditioning, data acquisition system (DAS) and image reconstruction system. This is illustrated in Figure 1

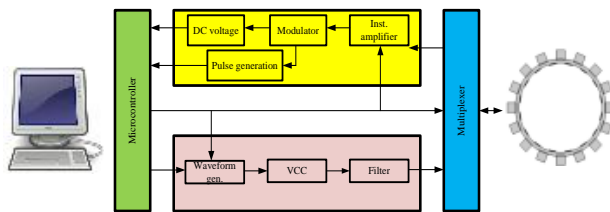


Figure 1 ERT system structure

2.0 SYSTEM OVERVIEW

In electrical resistance tomography (ERT) opposite excitation is applied to the electrodes and the resulting changing in voltages are measured. This method is less sensitive to conductivity change (as in adjacent strategy) as current flows through the centre point of the cross-section. This gives rise to even distribution of currents, leading to good image characterization [5] as illustrated in Figure 1. The number of independent current projections however is lower than for the adjacent strategy [6]. Based on current-voltage relationship the electrical properties of the conductivity distribution can be reconstructed. In the ERT system, the effective spatial resolution of the reconstructed images depends upon the number of elements in the FEM. Greater number of elements, the better the resolution. The number of independent measurements, depends upon the number of electrodes, N , should also be increased. In the adjacent measurement mode, the number of independent measurements (L) is given by the following equation:

$$L = \frac{N(N - 3)}{2} \tag{1}$$

where N is the number of electrodes. From Equation (1) for the 16 electrodes a total of 104 independent measurements can be obtained.

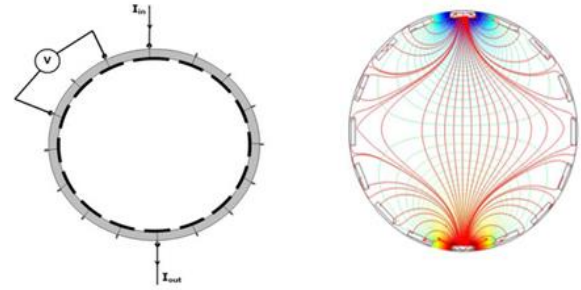


Figure 2 Opposite excitation strategy (a) Boundary potential measurements, (b) Equipotential and current density distribution

Table 1 Opposite measurement strategy of ERT for opposite excitation

Injection Pair	Ref.	Pair 1	Pair 2	Pair 3	Pair 4	Pair 5	Pair 6	Pair 7	Pair 8	Pair 9	Pair 10	Pair 11	Pair 12	Pair 13	Pair 14	Pair 15	Pair 16	No. Measurements
16-8	1	Ref	1-2	1-3	1-4	1-5	1-6	1-7	1-8	1-9	1-10	1-11	1-12	1-13	1-14	1-15	x	13
1-9	2	x	Ref	2-3	2-4	2-5	2-6	2-7	2-8	2-9	2-10	2-11	2-12	2-13	2-14	2-15	2-16	13
2-10	3	3-1	x	Ref	3-4	3-5	3-6	3-7	3-8	3-9	x	3-11	3-12	3-13	3-14	3-15	3-16	13
3-11	4	4-1	4-2	x	Ref	4-5	4-6	4-7	4-8	4-9	4-10	4-11	4-12	4-13	4-14	4-15	4-16	13
4-12	5	5-1	5-2	5-3	x	Ref	5-6	5-7	5-8	5-9	5-10	5-11	5-12	5-13	5-14	5-15	5-16	13
5-13	6	6-1	6-2	6-3	6-4	x	Ref	6-7	6-8	6-9	6-10	6-11	6-12	6-13	6-14	6-15	6-16	13
6-14	7	7-1	7-2	7-3	7-4	7-5	x	Ref	7-8	7-9	7-10	7-11	7-12	7-13	7-14	7-15	7-16	13
7-15	8	8-1	8-2	8-3	8-4	8-5	8-6	x	Ref	8-9	8-10	8-11	8-12	8-13	8-14	x	8-16	13
8-16	9	9-1	9-2	9-3	9-4	9-5	9-6	9-7	x	Ref	9-10	9-11	9-12	9-13	9-14	9-15	x	13
9-1	10	x	10-2	10-3	10-4	10-5	10-6	10-7	10-8	x	Ref	10-11	10-12	10-13	10-14	10-15	10-16	13
10-2	11	11-1	x	11-3	11-4	11-5	11-6	11-7	11-8	11-9	x	Ref	11-12	11-13	11-14	11-15	11-16	13
11-3	12	12-1	12-2	x	12-4	12-5	12-6	12-7	12-8	12-9	12-10	x	Ref	12-13	12-14	12-15	12-16	13
12-4	13	13-1	13-2	13-3	x	13-5	13-6	13-7	13-8	13-9	13-10	13-11	x	Ref	13-12	13-15	13-16	13
13-5	14	14-1	14-2	14-3	14-4	x	14-6	14-7	14-8	14-9	14-10	14-11	14-12	x	Ref	14-15	14-16	13
14-6	15	15-1	15-2	15-3	15-4	15-5	x	15-7	15-8	15-9	15-10	15-11	15-12	15-13	x	Ref	15-16	13
15-7	16	16-1	16-2	16-3	16-4	16-5	16-6	x	16-8	16-9	16-10	16-11	16-12	16-13	16-14	x	Ref	13
Total measurements:																		208

2.1 ERT Front-end Circuit

In the development of ERT system, it is important to have a stable current source with broad bandwidth and high output impedance. Howland current source (HCS) circuit is a well known high performance, voltage controlled current source (VCCS) which capable to provide high output impedance as well as high frequency bandwidth [7]. The HCS consists of an operational amplifier (op-amp) and several resistors. ERT system requires to inject a constant ac current to the pair of excitation electrode and measure the boundary potentials developed at the remaining surface electrodes. The ERT instrumentation, consists of voltage controlled current source (VCCS), switching module, signal conditioner module (SCM) and a data acquisition system (DAS) is used for boundary data collection. In this paper only VCCS and switching module are discussed.

2.2 Current Source

The modified Howland current pump circuit is shown in Figure 3. The voltage-controlled current source (VCCS) constructed from HCS provide current controlled excitation into load resistance which in case of conductive liquids. The design specification for current generator would have maximum current output of 10mA with maximum load of 1 kΩ. From Figure 3 the resistor (R_5) functions to increase output impedance while minimise the influence of the current source causes by variations of load resistance [8]. When $R_2 = R_3 = R_4$ and $R_1 = (R_2 + R_5)$ the output current can be calculated as follows:

$$I_{Load} = \frac{V_{input}}{R_5} \tag{2}$$

The Howland current pump was implemented to offer the best solution as it offers high performance and simplicity [9]. The VCCS in the proposed ERT system requires high output impedance, precision and stability over a wide frequency range between 1 kHz–500 kHz. Therefore the design is important part of the system. The current source in the ERT system must be able to deliver constant current over a frequency range between 1 kHz to 500 kHz, and be able to support load between 10 Ω to 1 kΩ. Hence the current source design should meet the specified above conditions. Assuming the perfect resistance matching among resistance used in the circuit, the output ideal impedance is infinite. However in practical implementation the output impedance become finite due to errors in resistances [10].

Equation (2) describe that using symmetrical resistors values in the circuit feedback scaling is larger than the load resistance. The transfer function also becomes easier and at the same time the input voltage is gained as well as voltage across resistor (R5). Three different types of high-speed operational amplifier (op-amp) were simulated which are LM7171, OPA604 and THS4061.

The resistor values with $R_2 = R_3 = R_5 = 600.2k\Omega$, $R_4 = 250\Omega$ and $R_1 = R_2 + R_4 = 600.45k\Omega \approx 600.5k\Omega$. All the resistors tolerance are 0.1%. From simulations it is found the high-speed, high output current LM7171 can be implemented in the circuit. The features of the LM7171: fast settling time (42 ns), high slew-rate 4100 V/us, wide gain bandwidth (200 MHz) and 100 mA output current [11]. The features is sufficient to produce current output between 1-10 mA between 1 kHz-500 kHz frequency range. General specification of the remaining devices is shown in Table 1 [11-13]. Figure 4 illustrates the recommended maximum input voltage for the tested devices must not exceed than 2.6 V before it saturated because of the rail-to-rail voltage. From Table 2 it is clearly showed the LM7171 op-amp is capable to provide high output impedance ($Z_o = 45.4k\Omega$) with load of 1 kΩ at maximum frequency of 500 kHz. Compared with the remaining op-amps which produces 7.0 kΩ and 2.5 kΩ for THS4061 and OPA604 respectively. The simulated output impedance results between 1 Hz to 10 MHz for all devices are shown in Figure 5. General specification of the remaining devices is shown in Table 2 while the simulated output impedance results between frequency 1 kHz to 10 MHz for these devices are shown in Table 3

Table 2 Specification of LM7171, OPA604 and THS4061 device

Specification	LM7171	THS4061	OPA604
Bandwidth	200MHz	180MHz	20MHz
Slew rate	4100V/us	400V/us	25V/us
Architecture	Voltage feedback	Voltage feedback	Voltage feedback
Output current	100mA	115mA	35mA

Table 3 Simulated output impedance of selected devices when frequencies varies between 1 kHz-1 MHz

Frequency (kHz)	LM7171	THS4061	OPA604
1	370.0kΩ	118.5kΩ	40.0kΩ
10	368.0kΩ	114.7kΩ	38.1kΩ
100	239.0kΩ	41.9kΩ	12.0kΩ
500	45.4k	7.0k	2.5k
1000	14.6kΩ	2.3kΩ	1.2kΩ

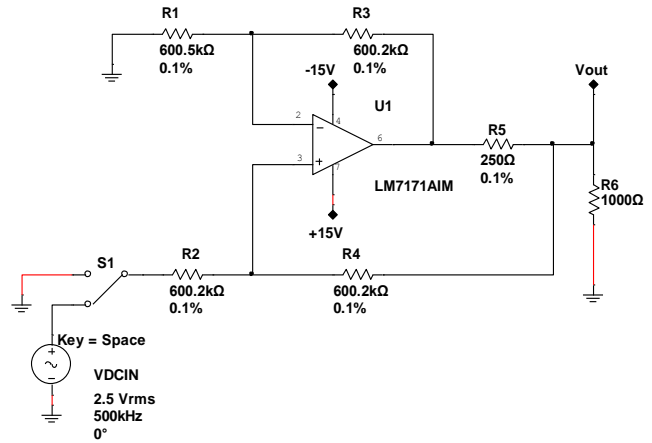


Figure 3 Voltage controlled current source (VCCS): Advanced Howland current pump

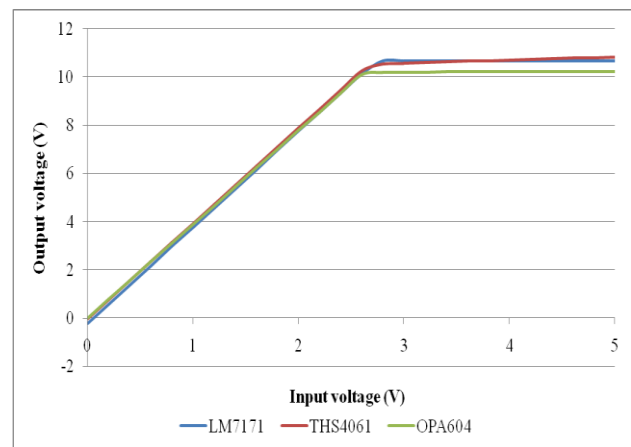


Figure 4 DC transfer characteristics

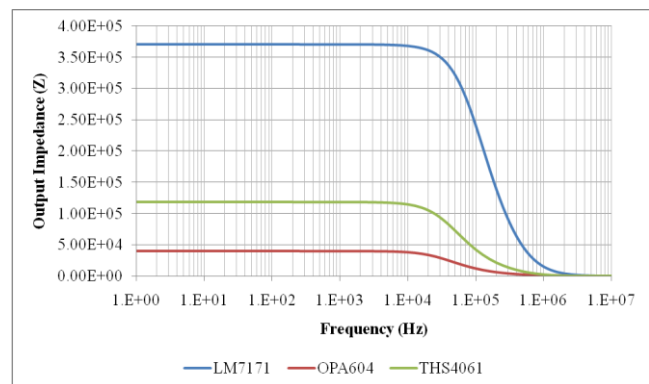


Figure 5 AC analysis with R_{load} 1 kΩ

Figure 6 shows the undistorted output current of 14.14 mA (peak) at 150 kHz and 500 kHz respectively using the LM7171.

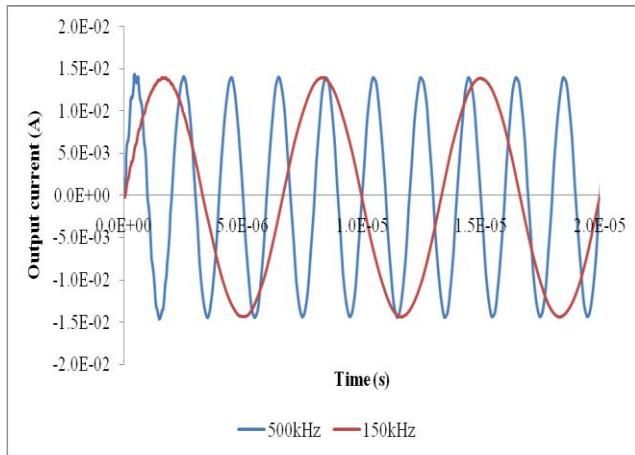


Figure 6 Output current from Howland current pump circuit

2.3 ERT Switching Module

The switching module is developed with high speed CMOS multiplexers. The switching module is developed using 16-channels analogue multiplexers (CD4067B) from Texas Instruments for 16-electrodes ERT system. The device selected due to its capability of producing low ON resistance typically (125 Ω) and short propagation delay by 30 ns [14]. During current excitation the ERT system requires two multiplexer (MUX-I_a and MUX-I_b) functions as current excitation switching and another two multiplexers (MUX-V_a and MUX-V_b) are used as measurement voltage switching. In the ERT system the parallel data bits are generated from microcontroller (DSPIC30F4012a) which is connected to the switching module. A total of 8-bit parallel data are required to controlled the current switching and voltage switching respectively. Figure 7 shows the switch arrangement of ERT switching module. The switching module was designed as each electrode functions in four different modes during its operation: excitation, ground, referenced and detection.

To avoid any signal losses during operation, selection of switching devices are important. The criteria of selected switches must have low on-state resistance (R_{on}), fast switching response, high-bandwidth, low charge injection and low crosstalk. Therefore switch device dual SPST TS5A2066 from Texas Instruments Inc. is selected because of its capability to have low on-state resistance, wide frequency response, low charge injection and cost effective. The general specification of dual SPST TS5A2066 is shown in Table 5 [15].

Table 5 General specification of TS5A2066

Parameter	Specification
On-resistance (R _{on})	7.5Ω
Bandwidth (BW)	400MHz
T _{on} / T _{off}	5.8ns / 3.6ns
Charge injection	1pC
Crosstalk	-66dB
Continuous current	+/-100mA

The switching arrangements of the four function modes are showed in Table 4"

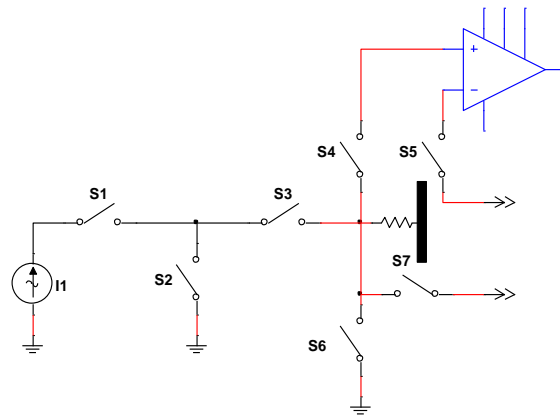


Figure 7 Switch arrangement in ERT system

Table 4 Four modes ERT electrode functions

Mode	Excitation	Ground	Reference	Detection
S1	•	o	o	o
S2	o	•	o	o
S3	•	o	o	o
S4	o	o	o	•
S5	o	o	o	•
S6	o	•	o	o
S7	o	o	•	o

• Switch close o Switch open

3.0 PRINCIPLE AND SIMULATION

Electrical resistance tomography (ERT) is a particular case of electrical impedance tomography (EIT). ERT is most widely and easily implemented for purely resistive medium [16]. ERT is based on the principles that different medium have different electrical properties. In ERT an electrical current is injected through a set of electrodes placed in a boundary of the domain of interest therefore resulting in an electrical field that is conditional by the conductivity distribution within the domain. The resulting electrical potential at the domain parameter can be measured using the remaining electrodes. For complete measurements or known as 1 scan is obtain when all electrodes are used for injection and differential potentials between all remaining pairs of adjacent electrodes are measured. When ERT is operated at low frequency (i.e 200 kHz) [17], only the electro-quasi-static (EQS) only the EQS needs to be considered. the ERT follows Equation (2).

$$\nabla \cdot (\sigma \nabla \phi) = 0, \quad \bar{r} \in \Omega \tag{3}$$

Electrodes, which are used to probe the object function as electrodes and electrode current flow measurement. Current is passed between the two electrodes and produce current patterns. At the same time other electrode serves as a measurement of the electrode potential difference with respect to the ground electrode. They are used to measure the voltage drop with a reference to the ground electrode. For the following boundary conditions the integral of current density across the electrode surface is equal to the current flow

$$\int_k \sigma \frac{\partial u}{\partial n} dS = I_k, \quad k = 1,2,3...K \tag{4}$$

For the part of object's surface under the current excitation electrodes the flows of current density has the form of:

$$\sigma \frac{\partial u}{\partial n} = j \quad (5)$$

For other surface of detection electrodes

$$\sigma \frac{\partial u}{\partial n} = 0 \quad (6)$$

Potential value, measured at the electrode is the sum of the potential on the surface under the electrode and the voltage drop on the contact resistance of the electrode:

$$u + Z_k \sigma \frac{\partial u}{\partial n} = U_k; k = 1, 2, 3 \dots K \quad (7)$$

where

ϕ = electric potential in the body

σ = conductivity

Z_k = contact impedance at k -th electrode

U = potential at k -th electrode

5.0 SIMULATION OF THE SENSING FIELD

The design process for the dual-modality sensor model consists of the following steps: geometry generation based to dimensions to be simulated, domain and boundary conditions properties and properties of physical conditions in sensor areas or zones. The design process for 16 ERT sensors can be divided into the following procedure:

- Selecting the study physics of the ERT which consists of electrical circuits and electrical current.
- Geometry modelling based on the dimension to be simulated.
- Set the boundary conditions and electrical properties for all domains or boundary.
- Generating the mesh. See Figure 8.
- Solve and find the field distribution
- Apply post-processing capabilities in COMSOL to calculate electrode voltages.

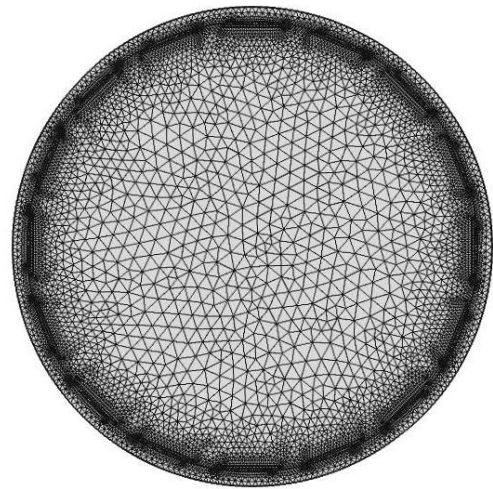


Figure 8 FEM meshing using extra fine mesh

In the simulation using COMSOL multiphysics the following parameters are used as shown in Table 6.

Table 6 Properties and physical parameters

No.	Item	Parameter
1.	Electrode material	Stainless steel
2.	Number of electrode plate	16
3.	Electrode width	12mm
4.	Inner diameter pipe	100mm
5.	Outer diameter pipe	105mm
6.	Excitation current	10mA
7.	Conductivity	0.3S/m

The system based on ERT with sine-wave current excitation was simulated with opposite excitation strategy. In order to effectively explain the potential distribution with variation of current excitation and frequency authors established a 2D simulation for 16-electrode ERT system accordingly with distribution of equi-potential lines and current density. According to Figure 8, we can see that the current density is sense where there is excitation electrode in the sensitivity field while sparse where the measurement electrode, which is similar with the distribution of equi-potential lines. The measurement result is directly proportional to the distribution of conductivity of mediums and the amplitude of excitation signals [18].

6.0 SIMULATION RESULT AND DISCUSSION

In Comsol current source excitation of 10 mA, at 150 kHz was simulated and injected to the excitation electrode pair and the surface potentials from the remaining electrodes are collected for the phantom configurations in homogeneous and non-homogeneous with air bubble as shown in Figure 9. The boundary potentials developed for homogeneous medium in Figure 10 shows that the surface potential profile varies in similar fashion as it changes from source to the ground electrode. It is also observed that the potential profiles of all the current projections are symmetric. It is also noticed that, for opposite method, only the first 120 voltages measured for first eight projections are independent to each other.

An air bubble with radius of 10 mm represents in-homogeneity located at boundary of the pipe wall. The bubble is

located near the electrode 7 (E7) and electrode 8 (E8). Current of 10 mA with 150 kHz was injected between pair E1 and E9. Figure 9(b) and 10(b) shows the potential distribution and boundary potentials when air bubble is at boundary. Boundary potential shows that several voltage peaks are significant at 7th and 8th electrode position. The pronounced potential is significant as the bubble located at the boundary. The result also presented that the boundary potentials is significantly influenced by bubble position particularly towards the boundary, higher potentials indicates that possible decrease of water conductivity because of presence bubble.

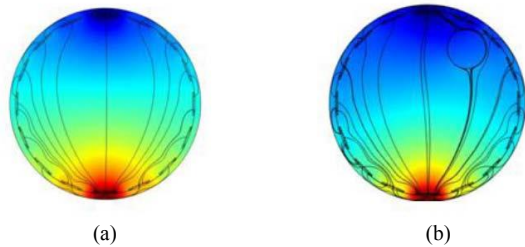


Figure 9 2D potential distribution of the ERT system using opposite strategy (a) Homogeneous medium, (b) Conductive medium with air bubble near boundary

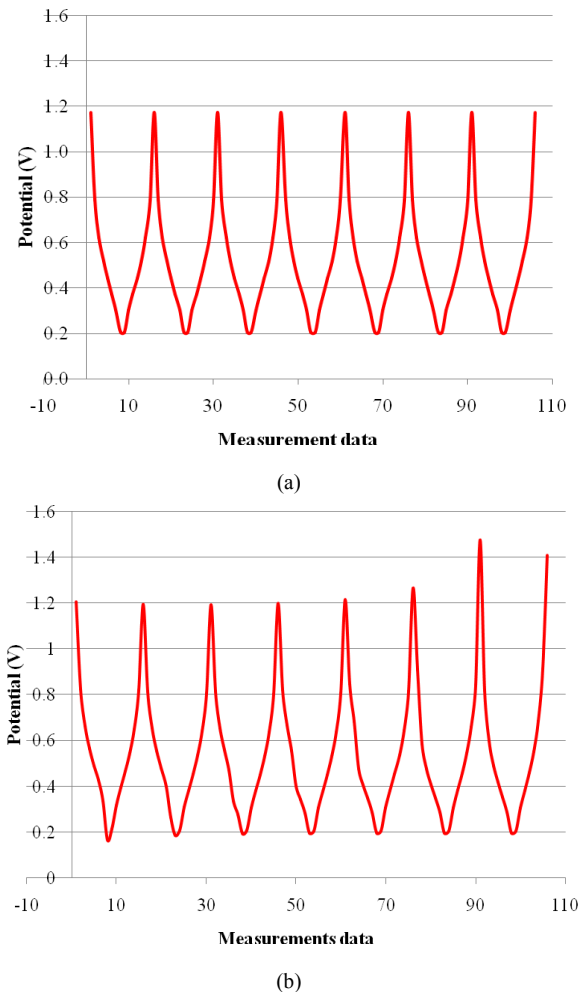


Figure 10 Boundary potentials of ERT system (a) Homogeneous medium, (b) Conductive medium with air bubble near boundary

7.0 CONCLUSION

In this paper, Howland current pump circuit has been studied to produce a constant ac current source with maximum 10 mA with frequency range between 1 kHz to 500 kHz. The LM7171 has been selected because of its capability to obtain high output impedance with load resistance of 1 k Ω . Opposite excitation current had also implemented and the results indicates that with such current amplitude of 10 mA and excitation strategy the ERT system capable for two phase liquid and gas distribution. From the simulation result the ERT is sensitive in bubble distribution detection in the medium particularly when the bubble is located near the boundary. The simulation results shows that the proposed front-end circuit can be potentially applied to two-phase liquid/gas flow.

Acknowledgement

The authors would like to thank the Public Service Department (JPA) of Malaysia and PROTOM-*i* group from Universiti Teknologi Malaysia (UTM) for supporting this work.

References

- [1] F. Ferraioli, A. Formisano, and R. Martone. 2005. A Circuitual Formulation for Direct Electrical Resistive Tomography Problems. *The International Journal for Computation and Mathematics in Electrical and Electronic Engineering*. 24: 11.
- [2] Jun-Wen Liu and F. Dong. 2004. Electrical Resistance Tomography Based on Single Drive Electrode Method. In *Proceedings of the Third International Conference on Machine Learning and Cybernetics, Shanghai*. 632–637.
- [3] C. Xu and F. Dong. 2011. Application of ERT System Measuring Oil/Water Two-phase Phase Flow Hold-up in Horizontal Pipe. Presented at the 4th International Workshop on Process Tomography, Chengdu China.
- [4] A. D. Okonkwo, M. Wang, and B. Azzopardi. Characterisation of a High Concentration Ionic Bubble Column Using Electrical Resistance Tomography. *Flow Measurement and Instrumentation*.
- [5] W. R. Breckon and M. K. Pidcock. 1987. Mathematical Aspects of Impedance Imaging. *Clinical Physics and Physiological Measurement*. 8: 77–84.
- [6] T. J. Yorkey and J. G. Webster. 1987. A Comparison of Impedance Tomographic Reconstruction Algorithms. *Clin. Phys. Physiol. Meas.* 8: 55–62.
- [7] H. Yazdani, M. M. Samani, and A. Mahanm. 2013. Characteristics of the Howland Current Source for Bioelectric Impedance Measurements Systems. In *Biomedical Engineering (ICBME), 2013 20th Iranian Conference on*. 189–193.
- [8] Z. Li, Z. Xu, C. Ren, W. Wang, D. Zhao, and H. Zhang. 2010. Study of Voltage Control Current Source in Electrical Impedance Tomography System. In *Bioinformatics and Biomedical Engineering (iCBBE), 2010 4th International Conference on*. 1–4.
- [9] M. Rafiei-Naeini and H. McCann. 2008. Low-noise Current Excitation Sub-system for Medical EIT. *Physiological Measurement*. 29: S173.
- [10] L. Jeong Whan, O. Tong In, P. Sang Min, L. Jae Sang, and W. Eung Je. 2003. Precision Constant Current Source for Electrical Impedance Tomography. In *Engineering in Medicine and Biology Society, 2003. Proceedings of the 25th Annual International Conference of the IEEE*. 2: 1066–1069.
- [11] LM7171-Very High Speed, High Output Current, Voltage Feedback Amplifier. T. Instruments, Ed. May 2013 ed: Texas Instruments Inc. 1993.
- [12] THS4061-180MHz High Speed Amplifier. T. I. Inc., Ed. December 2003 ed: Texas Instruments Inc. 1998.
- [13] OPA604 FET-Input, Low Distortion Operational Amplifier. T. I. Inc., Ed. September 2003 ed: Texas Instruments Inc.
- [14] CD4067-CMOS Analog Multiplexer/Demultiplexer. H. Semiconductor, Ed. ed: Texas Instruments Incorporated, June, 2003.
- [15] TS5A2066-DUAL-CHANNEL 10- Ω SPST ANALOG SWITCH. T. I. Inc., Ed. April 2010 ed: Texas Instruments Inc. 2005.

- [16] M. G. Rasteiro, R. Silva, F. A. P. Garcia, and P. Faia. 2011. Electrical Tomography: A Review of Configurations and Applications to Particulate Processes. *KONA Powder and Particle Journal*. 29: 67–80.
- [17] L. Yi and Y. Wuqiang. 2009. Measurement of Multi-phase Distribution Using An Integrated Dual-modality Sensor. In *Imaging Systems and Techniques, 2009. IST '09. IEEE International Workshop on*. 335–339.
- [18] P. Wang, B. Guo, and N. Li. 2009. Research on ERT System Denoising Technology Excited by Bi-directional Pulse Current. In *Control and Automation, 2009. ICCA 2009. IEEE International Conference on*. 1262–1265.